Tin clusters that do not melt: Calorimetry measurements up to 650 K

Gary A. Breaux, Colleen M. Neal, Baopeng Cao, and Martin F. Jarrold*
Department of Chemistry, Indiana University, 800 East Kirkwood Avenue, Bloomington, Indiana 47404, USA
(Received 25 September 2004; published 28 February 2005)

Recent theoretical studies [K. Joshi, D. G. Kanhere, and S. A. Blundell, Phys. Rev. B **67**, 235413 (2003)] predict that Sn_{20} melts at around 1200 K. We have performed calorimetry measurements on unsupported Sn_{18}^+, Sn_{19}^+, Sn_{20}^+, and Sn_{21}^+ in an effort to test this prediction. We find that these tin clusters disappear well below their predicted melting temperature due to dissociation. Calorimetry measurements performed up to around 650 K show some small features (which may be due to localized structural changes) but no clear melting transitions. Hence, tin clusters in this size regime do not melt—they sublime.

DOI: 10.1103/PhysRevB.71.073410 PACS number(s): 61.46.+w, 64.70.Dv

There has been interest in the melting of small particles for many years.[1–3] For particles with thousands of atoms, the melting point is depressed, due to the increase in the surface to volume ratio. For smaller particles (<500 atoms) size-dependent fluctuations in the melting temperatures have been observed.[4–6] In some cases, particles in the cluster size regime remain solid above the bulk melting point. This was first observed for tin.[7] Clusters with around 20 tin atoms adopt prolate geometries.[8] Hence, a transition to a spherical geometry (a liquid droplet) is an indicator for melting. However, when the temperature was raised to 50 K above the bulk melting point, the prolate geometry persisted, indicating that the clusters remain solid. Tin particles with thousands of atoms (either supported or embedded) show the usual melting point depression.[9–11] Measurements by Schäfer and coworkers[12] using a clusters beam indicate that the melting point depression extends down to particles with around 400 atoms. The location of the transition from depressed to elevated melting temperatures is currently unknown.

The elevated melting temperatures observed for small tin clusters are believed to have a structural origin. Density-functional molecular-dynamics (MD) simulations for Sn_{20} suggest that the lowest-energy structure, and the low-lying isomers, consist of two tricapped trigonal prism (TTP) units stacked end to end.[13] For a bulk material, melting is indicated by a spike in the heat capacity due to the latent heat. Heat capacities determined from the simulations for Sn_{20} show a small peak at around 500 K, a shoulder at around 850 K, and a broad maximum centered around 1200 K. The small peak and the shoulder were attributed to premelting transitions: rearrangements within the TTP units and distortion of one of the TTP units, respectively. While undergoing these transitions the Sn_{20} cluster retains its prolate shape. The large peak in the heat capacity centered at around 1200 K is due to melting: in the simulations, the two TTP units fuse to give a roughly spherical shape where the ionic cores undergo diffusive liquidlike motion. So the predicted melting temperature of Sn_{20} is around 700 K above the bulk melting point. There have been several theoretical studies of the melting of smaller tin clusters such as Sn_{10} and Sn_{13}, and the results suggest that they melt at higher temperatures than Sn_{20}.[14–16]

We have recently developed a method to determine the heat capacities of unsupported clusters.[17] The method is based on using multicollision-induced dissociation (MCID) to measure the dissociation threshold as a function of the clusters' initial temperature. As the temperature is increased, the dissociation threshold decreases due to the clusters' thermal energy. At the melting transition there is a sharp drop in the dissociation threshold due to the latent heat. This sharp drop, or the corresponding spike in the heat capacity (which is proportional to the derivative of the dissociation threshold), is a signature of melting. The interesting premelting transitions and the remarkably high melting temperature predicted for Sn_{20} prompted us to perform MCID calorimetry measurements on some tin clusters to examine the theoretical predictions. We found that Sn_{18}^+, Sn_{19}^+, Sn_{20}^+, and Sn_{21}^+ spontaneously fragment at well below the predicted melting temperature. Calorimetry measurements performed up to around 650 K show some small features but no clear melting transitions. Hence, tin clusters in this size regime do not melt—they sublime.

The tin cluster ions are created by laser vaporization of a liquid metal target in a cooled (253 K) helium buffer gas flow. Use of the liquid metal target provides more stable cluster signals than obtained with solid targets. A detailed description of the source will be provided elsewhere. The temperature of the clusters is set before they exit the source in a 10-cm-long temperature-variable extension. Two extensions are used to cover temperatures from 77 to 1200 K. The temperature of the extension is regulated to within around 1 K by microprocessor-based controllers. After exiting the extension, the ions are focused into a quadrupole mass spectrometer where a specific cluster size is selected. The size-selected cluster ions are then focused into a small collision cell that contains 1 Torr of helium. As the ions enter the collision cell, they undergo many collisions, each one converting a small fraction of the ions' translational energy into internal energy. The averaging inherent in this process yields a relatively narrow distribution of internal energies.[18] If the initial translational energy is high enough, the clusters can be heated to the point where they dissociate before their internal energies are cooled by further collisions with the helium. The undissociated cluster ions and the fragment ions are then swept across the collision cell by a weak electric field and a

fraction of them exit through a small aperture. The exiting ions are analyzed by a second quadrupole mass spectrometer and detected with an off-axis collision dynode and a microchannel plate assembly.

The tin clusters studied here (Sn_{18}^+, Sn_{19}^+, Sn_{20}^+, and Sn_{21}^+) generate "fission" products rather than undergoing the evaporation of individual atoms that is characteristic of metal clusters. The observed dissociation pathways are

$$Sn_{18}^+ \rightarrow Sn_{11}^+ + Sn_7;$$

$$Sn_{19}^+ \rightarrow Sn_9^+ + Sn_{10}(\sim 73\%), \quad Sn_{10}^+ + Sn_9(\sim 16\%),$$

$$Sn_{12}^+ + Sn_7(\sim 11\%);$$

$$Sn_{20}^+ \rightarrow Sn_{10}^+ + Sn_{10}; \text{ and}$$

$$Sn_{21}^+ \rightarrow Sn_{11}^+ + Sn_{10};$$

which are independent of the temperature of the extension. These pathways are very similar to those observed by Tai and coworkers,[19] who performed fragmentation studies of tin clusters Sn_n^+ ($n=4-20$) by low-energy collisions with highly oriented pyrolytic graphite.

The fraction of the ions that dissociate on entering the collision cell is obtained from the mass spectra. The ions' translational energy is varied, and the fraction that dissociate is determined as a function of the translational energy. The translational energy required for 50% of the ions to dissociate (TE50%D) is then determined from an interpolation. This quantity, TE50%D, is then measured as a function of the temperature of the source extension. A plot of TE50%D for Sn_{18}^+, Sn_{19}^+, Sn_{20}^+, and Sn_{21}^+ is shown in Fig. 1(a). The values for Sn_{19}^+ are systematically larger than for the other clusters, which indicates that this cluster has enhanced stability towards dissociation. In all cases, the TE50%D values decrease relatively smoothly as the temperature is raised. This decrease can be attributed to the increase in the internal energy of the clusters due to their heat capacities. A localized steeper drop in the TE50%D values (which results from the latent heat) is a signature of melting. There is no such drop evident in the results shown in Fig. 1(a).

The derivative of TE50%D with respect to temperature ($-\partial \mathrm{TE50\%D}/\partial T$) is approximately proportional to the heat capacity of the cluster. The proportionality constant is the fraction of the clusters' translational energy that is converted into internal energy as they collide with helium in the collision cell. This quantity can be estimated from a simple impulsive collision model.[18] Previous work indicates that this approach is reliable.[17,20] The fraction of the ions' translational energy converted into internal energy is small (around 0.012) because the collision partner (helium) is so light. The small value for this quantity is a key feature of the method, because small changes in the internal energy of the clusters lead to large changes in the translational energy required to cause 50% of the ions to dissociate (TE50%D). The heat capacities determined from the TE50%D values are shown in Fig. 1(b). These points are the average of at least two (and in most cases three or more) independent measurements. The heat capacities are normalized to $3Nk$ (the classical heat capacity), where k is the Boltzmann constant and $N=3n-6+3/2$ with $n=$number of atoms in the cluster. The dashed lines represent the heat capacities calculated using statistical thermodynamics: the vibrational component is obtained from a modified Debye model that incorporates a low-frequency cutoff to account for the finite size of the clusters[21] and the rotational component is treated classically. The measured heat capacities appear to be systematically below the classical values. This could be caused by an underestimate of the fraction of the ions' translational energy that is converted into internal energy; although, the approach employed here appeared to be accurate in previous studies.[17,20] The heat capacity measurements were only performed up to around 650 K because the cluster signals disappear at higher temperatures. All the heat capacities appear to decrease slightly at the upper end of the range studied. This drop could be an artifact related to the disappearance of the signal. Close to the dissociation temperature, the clusters that survive and

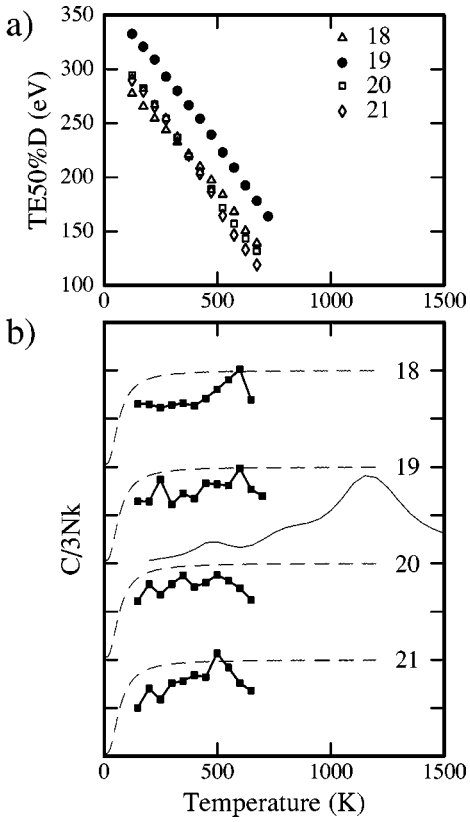

FIG. 1. (a) Shows TE50%D plotted against the temperature of the extension for Sn_{18}^+, Sn_{19}^+, Sn_{20}^+, and Sn_{21}^+. (b) Shows plots of the heat capacities determined from the derivative of TE50%D with respect to temperature. The heat capacities are normalized to $3Nk$ (the classical heat capacity) where k is the Boltzman constant and $N=3n-6+3/2$, with $n=$number of atoms in the cluster. The dashed lines show the heat capacity calculated using statistical thermodynamics: the vibrational component is calculated using a modified Debye model (see text) and the rotational component is treated classically. The thin solid line shows the heat capacities calculated for Sn_{20} by Joshi *et al.* (Ref. 13).

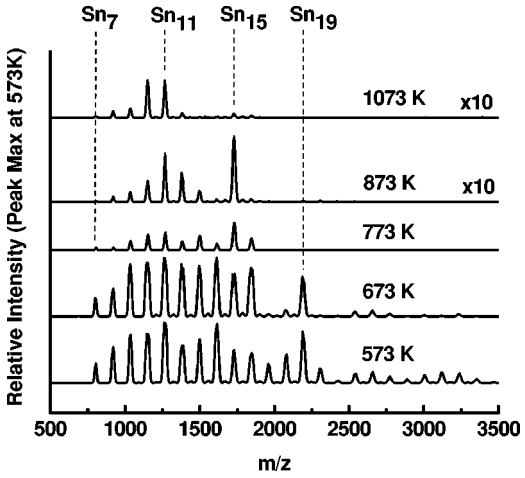

FIG. 2. Mass spectra recorded for tin clusters as a function of the source extension temperature for temperatures between 573 K to 1073 K. The translational energy was 150 eV. Note that the spectra at 873 K and 1073 K are $\times 10$.

exit the extension intact will be the ones with low internal energies. This distortion of the internal energy distribution of the clusters which reach the collision cell could lead to artificially depressed values for the heat capacities.

The heat capacity for Sn_{18}^+ is initially low and then rises to peak at around 600 K before falling sharply, possibly for the reason mentioned above. It is possible that the initial increase represents the beginning of a melting or premelting transition. There are two reproducible maxima in the heat capacity of Sn_{19}^+ at around 250 and 600 K. The heat capacity for Sn_{20}^+ varies little as a function of temperature, while that for Sn_{21}^+ shows a small reproducible peak at around 500 K.

As indicated above, the tin cluster ions studied here vanish as the extension temperature is raised above around 650 K. The source temperature is maintained at 253 K as the temperature of the extension is varied. We have generated large tin clusters with a source employing similar conditions but without the extension, so there is no doubt that the disappearance of the clusters studied here is related to their thermally activated dissociation in the heated extension. Figure 2 shows a plot of the mass spectra recorded for the tin clusters that exit the extension as a function of temperature. Mass spectra measured below 573 K do not change significantly and so they are not shown. As the temperature is raised, clusters with $n > 16$ diminish and disappear. Sn_{19}^+ survives to a slightly higher temperature than the other clusters, indicating that this cluster is slightly more stable than its neighbors, an observation consistent with the results shown in Fig. 1(a). Above 700 K, Sn_{15}^+ is the most abundant cluster. Only Sn_{10}^+ and Sn_{11}^+ display sufficient stability to survive in significant abundance above 1000 K.

The thin solid line in Fig. 1(b) shows the heat capacities calculated for Sn_{20}.[13] The broad maximum centered around 1200 K is the calculated melting transition while the small peak at 500 K and the shoulder at 850 K are the premelting transitions mentioned above. The peak at 500 K was attributed to rearrangement processes within the TTP units. While the cluster ions studied here clearly dissociate well before they reach the predicted melting temperature, there is some overlap between the measured and calculated heat capacities. However, there is no compelling evidence in the experimental measurements for Sn_{20}^+ for the small peak in the calculated heat capacities at around 500 K. On the other hand, the predicted peak is small and may well be lost within the uncertainty of our measurements. There are small maxima in the measured heat capacities for the other clusters at close to 500 K, which may result from premelting transitions due to localized structural changes along the lines found in the simulations for Sn_{20}.

The MD simulations were performed on neutral Sn_{20} while the measurements were done on cluster ions. This could certainly provide an explanation for the apparent absence of the premelting peak at 500 K (the peak could be smaller for the ion or shifted to a slightly higher temperature). On the other hand, the charge state should not dramatically alter the relative stability of the clusters, so if the ions dissociate on the experimental time scale at around 650–750 K the neutral clusters are not expected to behave very differently. Comparison with DFT calculations shows that the fission processes observed here and in the surface dissociation experiments occur because they generate the lowest-energy fragments.[19,22] In other words, Sn_{20} dissociates to two Sn_{10} units because the Sn_{10} cluster (a tricapped trigonal prism) is particularly stable. The DFT calculations indicate that almost 90% of the bulk cohesive energy is recovered by Sn_{10},[22] a much larger fraction than is expected for a typical metal cluster. Because of the high stability of the Sn_{10} units, the dissociation energy of Sn_{20} is relatively low, and so Sn_{20} dissociates before it melts; in other words, this cluster sublimes. Interestingly, bulk tin, which melts at 505 K, has a remarkably wide liquid range for an element with such a low melting point: its boiling point is 2875 K.

As a final note we point out that the formation of "magic" fragments, like the Sn_{10} cluster that dominates the fragmentation products of medium-sized tin clusters, provides a strong indication that dissociation is occurring from a solid cluster. "Magic" clusters, like Sn_{10}, are particularly stable because they adopt a favorable geometry. In the liquid cluster there should be no preference for a particular geometry, and so liquid clusters that dissociate (to give liquid products) should not generate "magic" fragments. Liquid clusters should dissociate by loss of individual atoms, as is usually observed in the dissociation of metal clusters.

We gratefully acknowledge the support of this work by the National Science Foundation.

*Corresponding author. Email address: mfj@indiana.edu

[1] P. Z. Pawlow, Phys. Chem. **65**, 1 (1909).
[2] M. J. Takagi, J. Phys. Soc. Jpn. **9**, 359 (1954).
[3] Ph. Buffat and J. P. Borel, Phys. Rev. A **13**, 2287 (1976).
[4] M. Schmidt, R. Kusche, B. von Issendorff, and H. Haberland, Nature (London) **393**, 238 (1998).
[5] M. Schmidt and H. Haberland, C. R. Phys. **3**, 327 (2002).
[6] G. A. Breaux, D. A. Hillman, C. M. Neal, R. C. Benirschke, and M. F. Jarrold, J. Am. Chem. Soc. **126**, 8628 (2004).
[7] A. A. Shvartsburg and M. F. Jarrold, Phys. Rev. Lett. **85**, 2530 (2000).
[8] A. A. Shvartsburg and M. F. Jarrold, Phys. Rev. A **60**, 1235 (1999).
[9] S. L. Lai, J. Y. Guo, V. Petrova, G. Ramanath, and L. H. Allen, Phys. Rev. Lett. **77**, 99 (1996).
[10] C. E. Bottani, A. Li Bassi, B. K. Tanner, A. Stella, P. Tognini, P. Cheyssac, and R. Kofman, Phys. Rev. B **59**, R15 601 (1999).
[11] L. E. Deparo, E. Bontempi, L. Sangaletti, and S. Pagliara, J. Chem. Phys. **118**, 1400 (2003).
[12] T. Bachels, H.-J. Güntherodt, and R. Schafer, Phys. Rev. Lett. **85**, 1250 (2000).
[13] K. Joshi, D. G. Kanhere, and S. A. Blundell, Phys. Rev. B **67**, 235413 (2003).
[14] Z.-Y. Lu, C.-Z. Wang, and K.-M. Ho, Phys. Rev. B **61**, 2329 (2000).
[15] K. Joshi, D. G. Kanhere, and S. A. Blundell, Phys. Rev. B **66**, 155329 (2002).
[16] F.-C. Chuang, C. Z. Wang, S. Öğüt, J. R. Chelikowsky, and K. M. Ho, Phys. Rev. B **69**, 165408 (2004).
[17] G. A. Breaux, R. C. Benirschke, T. Sugai, B. S. Kinnear, and M. F. Jarrold, Phys. Rev. Lett. **91**, 215508 (2003).
[18] M. F. Jarrold and E. C. Honea, J. Phys. Chem. **95**, 9181 (1991).
[19] Y. Tai, J. Murakami, C. Marumder, V. Kumar, H. Mizuseki, and Y. Kawazoe, J. Chem. Phys. **117**, 4317 (2002).
[20] J. M. Hunter, J. L. Fye, M. F. Jarrold, and J. E. Bower, Phys. Rev. Lett. **73**, 2063 (1994).
[21] J. Bohr, Int. J. Quantum Chem. **84**, 249 (2001).
[22] C. Majumder, V. Kumar, H. Mizuseki, and Y. Kawazoe, Phys. Rev. B **64**, 233405 (2001).